Soliton polarization dynamics in fiber lasers passively mode-locked by the nonlinear polarization rotation technique

J. Wu,[1] D. Y. Tang,[2] L. M. Zhao,[2] and C. C. Chan[1]
[1]*School of Chemical and Biomedical Engineering, Nanyang Technological University, Singapore 639798*
[2]*School of Electrical and Electronic Engineering, Nanyang Technological University, Singapore 639798*
(Received 4 May 2006; revised manuscript received 12 August 2006; published 6 October 2006)

By numerically solving the coupled laser Ginzburg-Landau equations and using the pulse tracing technique to incorporate the cavity effect in the simulation, we have explicitly calculated the soliton polarization ellipses throughout the cavity of a fiber-ring laser mode-locked by the nonlinear polarization rotation technique, and investigated the soliton polarization dynamics in laser cavities. It was found that in a conventional stable soliton operation state, although the soliton polarization varies as the pulse propagates, at a fixed position inside the laser cavity the soliton polarization is invariant with time. However, in the presence of laser dynamics, at a fixed location within the cavity the soliton could either have multiple alternating fixed polarization states or no fixed polarization state at all, depending on the soliton dynamics.

DOI: 10.1103/PhysRevE.74.046605 PACS number(s): 42.65.Tg, 05.45.Yv, 42.79.−e, 05.45.−a

I. INTRODUCTION

Passively mode-locked soliton fiber lasers as an alternative source of ultrashort optical pulses have been extensively investigated [1–4]. Various passive mode-locking techniques such as the nonlinear loop mirror, the semiconductor saturable absorber (SESAM), and the nonlinear polarization rotation (NPR) have been used to achieve the self-started soliton operation of lasers. In particular, due to its simplicity and ease of implementation, the NPR method was widely used and theoretically intensively studied [5–8]. The NPR technique takes advantage of the weak birefringence of single-mode fibers to generate a fast artificial saturable absorber effect, which initiates the mode locking, and after the soliton is formed, further stabilizes the soliton operation through suppressing the cavity background-noise generation. Despite the fact that standard single-mode optical fibers commonly used for the construction of fiber lasers support two orthogonal polarization modes, soliton propagation in laser cavities is often treated as a scalar problem and the vector nature of the wave is ignored. This approach is rigorous only if the fiber is truly isotropic. However, in reality the fiber is always slightly birefringent due to structure asymmetry, strain, bending, etc. The presence of birefringence lifts the degeneracy between the two modes, resulting in differences in both phase and group velocities [9,10]. Although it was recently shown that for a passively mode-locked fiber laser with very weak cavity birefringence, phase locking between the two polarization modes could be achieved and consequently, the vector soliton with its polarization state maintained during the propagation could be formed in laser cavities [11,12]. Obviously, in the NPR mode-locked fiber lasers the phases between the two modes can never be locked. Thus it is worth investigating how the polarization state of the vector solitons formed in these lasers evolves. On the other hand, it was both experimentally and numerically demonstrated that under certain conditions the soliton emission of the fiber lasers can exhibit period-doubling bifurcation and a period-doubling route to chaos [13,14]. A period-doubling route to chaos is a typical characteristic of nonlinear dynamic systems when they transit from stable states to chaotic states. Hence it would also be interesting to know the impact of the laser dynamics on the soliton polarization evolution in the cavity.

We note that the polarization dynamics of vector solitons in birefringent fibers have already been investigated previously [15–19]. Although the results of this research to some extent gives an insight into the soliton polarization dynamics in birefringent laser cavities, the soliton circulation in laser cavities is inherently different from the soliton propagation in optical fibers. It is because a soliton circulating in a laser cavity is subject to periodic perturbation by cavity components such as polarizer and polarization controllers, and the system is nonconservative with the circulation accompanied by periodic amplification and dissipation of the optical field. To determine the distinct features of the polarization dynamics of soliton circulation inside laser cavities, we conducted a comprehensive numerical study on the soliton polarization evolution in fiber-ring lasers passively mode-locked by the NPR technique, taking into account all the possible influence factors, especially those that distinguish the soliton circulation in laser cavities from the soliton propagation in optical fibers.

II. FIBER-RING LASER MODEL

A schematic of the fiber laser system modeled is shown in Fig. 1 below. The cavity consists of one piece of 4-m-long erbium-doped fiber (EDF) with group-velocity dispersion (GVD) β_2 equal to -10 ps/km^2 and two pieces of 1-m-long dispersion-shifted fiber (DSF) with $\beta_2=-2$ ps/km^2 connected at both ends of the EDF. Other cavity elements include one output coupler with a coupling ratio of $0.9^2/(1-0.9^2)=0.81/0.19$, one polarization controller (PC), and one polarization-dependent isolator (PI). As the cavity is a ring, the PI plays the roles of both the polarizer, transforming an arbitrarily polarized light into a linearly polarized one, and the analyzer, introducing an intensity-dependent transmittance (loss) to realize the fast artificial saturable absorber effect so as to achieve passive mode locking [5]. When light

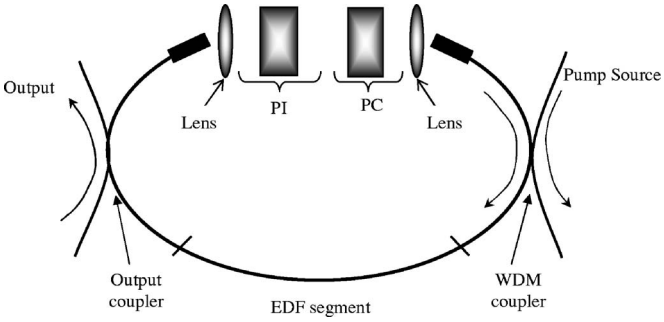

FIG. 1. The fiber-ring laser system modeled.

is incident on a piece of single-mode fiber, it splits into two polarization modes along the orthogonal principal axes of the fiber. For the simplicity of calculation, we have assumed that the principal axes of the different pieces of fibers in the cavity coincide.

We note that Salhi *et al.* have theoretically studied the influence of noncoincidence of the axes on the laser operation [20]. It turned out that it affects only the area of the mode-locking domains in the parameter space rather than the soliton laser dynamics as is evident from the governing equations. Therefore we adopted the assumption to simplify the numerical model. Actually, the effect caused by the possible noncoincidence of the fiber principal axes has been implicitly considered in our model. It is accounted for by the PC inserted in the cavity, which introduces a phase difference (linear phase delay bias) between the two polarization components. Inside the optical fibers the light will experience the linear birefringence of the fibers and the nonlinear birefringence arisen from the self-phase modulation (SPM) and the cross-phase modulation (XPM), thus the polarization ellipse of the light will normally rotate as it propagates. Depending on the birefringence strength of the fibers, wave mixing between the orthogonal polarization components may also play a role in the soliton polarization evolution.

Nonlinear wave propagation in a piece of linearly birefringent fiber is well described by the coupled nonlinear Schrödinger equations (NLSE) [9]

$$\frac{\partial A_x}{\partial Z} + \delta\frac{\partial A_x}{\partial T} + \beta_2\frac{j}{2}\frac{\partial^2 A_x}{\partial T^2} - \frac{\beta_3}{6}\frac{\partial^3 A_x}{\partial T^3} = j\gamma\left(|A_x|^2 + \frac{2}{3}|A_y|^2\right)A_x + j\frac{\gamma}{2}A_x^* A_y^2 \exp[-j2\Delta\beta z], \quad (1)$$

$$\frac{\partial A_y}{\partial Z} + \delta\frac{\partial A_y}{\partial T} + \beta_2\frac{j}{2}\frac{\partial^2 A_y}{\partial T^2} - \frac{\beta_3}{6}\frac{\partial^3 A_y}{\partial T^3} = j\gamma\left(|A_y|^2 + \frac{2}{3}|A_x|^2\right)A_y + j\frac{\gamma}{3}A_y^* A_x^2 \exp[+j2\Delta\beta z]. \quad (2)$$

In the above equations,

$$\beta_x(\omega) = \beta_{0x} + \beta_{1x}(\omega-\omega_0) + \frac{1}{2}\beta_{2x}(\omega-\omega_0)^2 + \frac{1}{6}\beta_{3x}(\omega-\omega_0)^3 \ldots,$$

$$\beta_y(\omega) = \beta_{0y} + \beta_{1y}(\omega-\omega_0) + \frac{1}{2}\beta_{2y}(\omega-\omega_0)^2 + \frac{1}{6}\beta_{3y}(\omega-\omega_0)^3 \ldots,$$

$$\Delta\beta = \beta_{0x} - \beta_{0y} = \frac{2\pi}{\lambda}B_m = \frac{2\pi}{L_B},$$

which is related to the birefringence of the fiber. Moreover, the GVD parameter β_2, the third-order dispersion (TOD) parameter β_3, and the nonlinear coefficient γ for the two polarization modes are the same if they have the same central wavelength λ_0, which was always assumed in the simulations. A_x and A_y are normalized slow-varying envelopes of the electric fields polarized along the two principal axes (denoted as the x and y axes, where the x axis is the slow axis) of the birefringent fiber, and $\delta=(\beta_{1x}-\beta_{1y})/2$ is the linear group-velocity difference between the two polarization modes. T and Z are the time and space coordinates referring to a retarded reference frame moving at a velocity equal to the average of the linear group velocities along the x and y axes, which are defined as $T=t-z/v_g=t-[(\beta_{1x}+\beta_{1y})/2]z$ and $Z=z$, respectively.

Define $A_x=F_h\exp(-j\Delta\beta z/2)$ and $A_y=F_v\exp(+j\Delta\beta z/2)$. Substitute them into Eqs. (1) and (2). After some simple algebra, we obtain

$$\frac{\partial F_h}{\partial Z} - j\frac{\Delta\beta}{2}F_h + \delta\frac{\partial F_h}{\partial T} + \beta_2\frac{j}{2}\frac{\partial^2 F_h}{\partial T^2} - \frac{\beta_3}{6}\frac{\partial^3 F_h}{\partial T^3} = j\gamma\left(|F_h|^2 + \frac{2}{3}|F_v|^2\right)F_h + j\frac{\gamma}{3}F_h^* F_v^2, \quad (3)$$

$$\frac{\partial F_v}{\partial Z} + j\frac{\Delta\beta}{2}F_v - \delta\frac{\partial F_v}{\partial T} + \beta_2\frac{j}{2}\frac{\partial^2 F_v}{\partial T^2} - \frac{\beta_3}{6}\frac{\partial^3 F_v}{\partial T^3} = j\gamma\left(|F_v|^2 + \frac{2}{3}|F_h|^2\right)F_v + j\frac{\gamma}{3}F_v^* F_h^2. \quad (4)$$

For birefringent EDF, nonlinear wave propagation is described by the coupled Ginzburg-Landau equations [21]

$$\frac{\partial F_h}{\partial Z} = j\frac{\Delta\beta}{2}F_h - \delta\frac{\partial F_h}{\partial T} - \beta_2\frac{j}{2}\frac{\partial^2 F_h}{\partial T^2} + \frac{\beta_3}{6}\frac{\partial^3 F_h}{\partial T^3} + j\gamma\left(|F_h|^2 + \frac{2}{3}|F_v|^2\right)F_h + j\frac{\gamma}{3}F_h^* F_v^2 + \frac{g_p(T)}{2}F_h + \frac{g_p(T)}{2.\Omega_g^2}\frac{\partial^2 F_h}{\partial T^2}, \quad (5)$$

$$\frac{\partial F_v}{\partial Z} = -j\frac{\Delta\beta}{2}F_v + \delta\frac{\partial F_v}{\partial T} - \beta_2\frac{j}{2}\frac{\partial^2 F_v}{\partial T^2} + \frac{\beta_3}{6}\frac{\partial^3 F_v}{\partial T^3} + j\gamma\left(|F_v|^2 + \frac{2}{3}|F_h|^2\right)F_v + j\frac{\gamma}{3}F_v^* F_h^2 + \frac{g_p(T)}{2}F_v + \frac{g_p(T)}{2.\Omega_g^2}\frac{\partial^2 F_v}{\partial T^2}, \quad (6)$$

where the new terms $[g_p(T)/2]Fh$ and $[g_p(T)/2]Fv$ account for the gain provided by the EDF whereas the terms $[g_p(T)/2\Omega_g^2](\partial^2 Fh/\partial T^2)$ and $[g_p(T)/2\Omega_g^2](\partial^2 Fv/\partial T^2)$ represent the gain dispersion of the EDF.

$g_p(t)$, the saturable gain in Eqs. (5) and (6), is defined as

$$g_p(t) = g_o \exp\left[-\frac{1}{E_s}\int_{-\infty}^{t}(|F_h|^2 + |F_v|^2)dt'\right],$$

where g_o refers to the small signal gain, Ω_g refers to the gain bandwidth, and E_s is the saturation energy, which has a typical value of 1 μJ.

Equations (3)–(6) are now ready to be solved numerically by the standard symmetrized split-step Fourier method. To also take into account the effects of the cavity components and the laser cavity, we further used a so-called pulse-tracing technique to simulate the soliton evolution in the cavity [8]. The main idea of the technique is that we follow the circulation of the soliton in the cavity and consider the action of every cavity component on the soliton. The propagation of the soliton in various pieces of fiber is described by either the coupled nonlinear Schrödinger equations (for undoped fibers) or the coupled Ginzburg-Landau equations (for doped fibers) as given above. The functions of discrete cavity components such as polarizers and polarization controllers are modeled by 2×2 transfer matrices and their actions on the optical wave are simulated by multiplying the light field with their respective transfer matrices when the soliton encounters them in the cavity. As this treatment is very similar to the ray tracing by the matrix technique in geometrical optics and the *ABCD* law in Gaussian beam optics, we termed it "pulse tracing." This technique assures that the obtained numerical results satisfy the laser cavity resonant condition.

III. DETERMINATION OF THE SOLITON POLARIZATION STATE

The polarization state of a continuous wave (CW) is determined by the pattern traced out by the electric-field vector tip as a function of time in a fixed transverse plane (fixed space view). In the context of optical pulses, this method is still applicable if the pulse width is broad enough compared with one cycle of the carrier frequency. For the soliton pulses obtained in the passively mode-locked fiber lasers this condition is well satisfied. Therefore, we used the same method to determine the polarization states of the soliton pulses. The two polarization modes of a vector soliton can be written as

$$\vec{\mathbf{E}}_{\mathbf{x}}(z,t) = \hat{x}|Fh(z,t)|\cos[\bar{\beta}_0 z - \omega_0 t + \phi h(z,t)], \quad (7)$$

$$\vec{\mathbf{E}}_{\mathbf{y}}(z,t) = \hat{y}|Fv(z,t)|\cos[\bar{\beta}_0 z - \omega_0 t + \phi v(z,t)], \quad (8)$$

where $\bar{\beta}_0 = \frac{1}{2}(\beta_{0x} + \beta_{0y})$ is the average of the wave numbers; ϕh and ϕv are the phases of Fh and Fv, respectively.

In the context of laser cavities due to the effects of cavity gain and gain dispersion, the solitons formed are generally chirped. Therefore, the phases ϕh and ϕv vary with time. Frequency chirp of a pulse causes polarization nonuniformity across the pulse envelope. In our numerical simulations we have calculated the frequency chirps of the soliton at different cavity locations. It turned out that not only the chirp was small (the maximum frequency shift $\Delta\omega$ within the FWHM pulse width was no more than 0.66% of the carrier frequency for the maximum pumping strength we chose) but also at a fixed location in the cavity the chirp was fixed, i.e., it did not vary with the number of round-trips the soliton had propagated. It was generally believed that because of their intensity difference, the peak and wing of a pulse formed in the lasers passively mode-locked by the NPR technique will have different polarization rotations and thus will experience different attenuation by the intracavity polarizer. However, our numerical studies show that when the mode-locked pulse has evolved into a soliton, it has uniform polarization across the pulse profile. Hence the soliton polarization could simply be represented by the polarization state of any point in the soliton pulse envelope. We therefore used the amplitudes and phases of the two polarization components at the pulse envelope peaks (the group velocities of the two polarization modes are always locked together, hence their pulse envelope peaks coincide) to construct the instantaneous electrical-field vector. The contour traced out by the combined electrical-field vector tip was then the polarization ellipse of the optical pulse at a position.

IV. SOLITON POLARIZATION EVOLUTION IN A CAVITY

Figure 2 depicts the soliton polarization evolution inside a laser whose cavity length is equal to the beat length, i.e., $L = L_B$, under a stable single-pulse soliton operation. The light after passing through the PC is elliptically polarized. As it traverses further in the fibers, its polarization state varies. Both the ellipticity and orientation of the polarization ellipse change during the propagation. After one cavity length the polarization ellipse makes a complete round of rotation (the phase difference between the two polarization modes changes by about 2π). At a fixed position in the cavity, the polarization state of the soliton is fixed, which is invariant with time.

Keeping all the other cavity parameters unchanged, the fiber beat length was varied to $L/L_B=2$, $L/L_B=3$, and $L/L_B=4$. Similar soliton polarization state evolutions were obtained, except that in those cases the number of rounds of the polarization ellipse rotation completed over one cavity length were different, which is close to the respective ratio of the cavity length over the beat length. The soliton polarization state evolution along the cavity is caused by both the linear and nonlinear birefringence with the former dominating over the latter according to the numerically calculated results. For a close examination of their relative strength, we calculated the phase difference between the two polarization components accumulated in one cavity round-trip for various strengths of the linear birefringence and tabulated in Table I. The "+" signs in Table I indicate that the nonlinear polarization rotation added up to the linear polarization rotation. In the practice, whether the nonlinear polarization rotation adds up to or opposes the linear polarization rotation depends on the specific orientation of the polarizer, namely, whether it makes the light polarization component along the slow axis

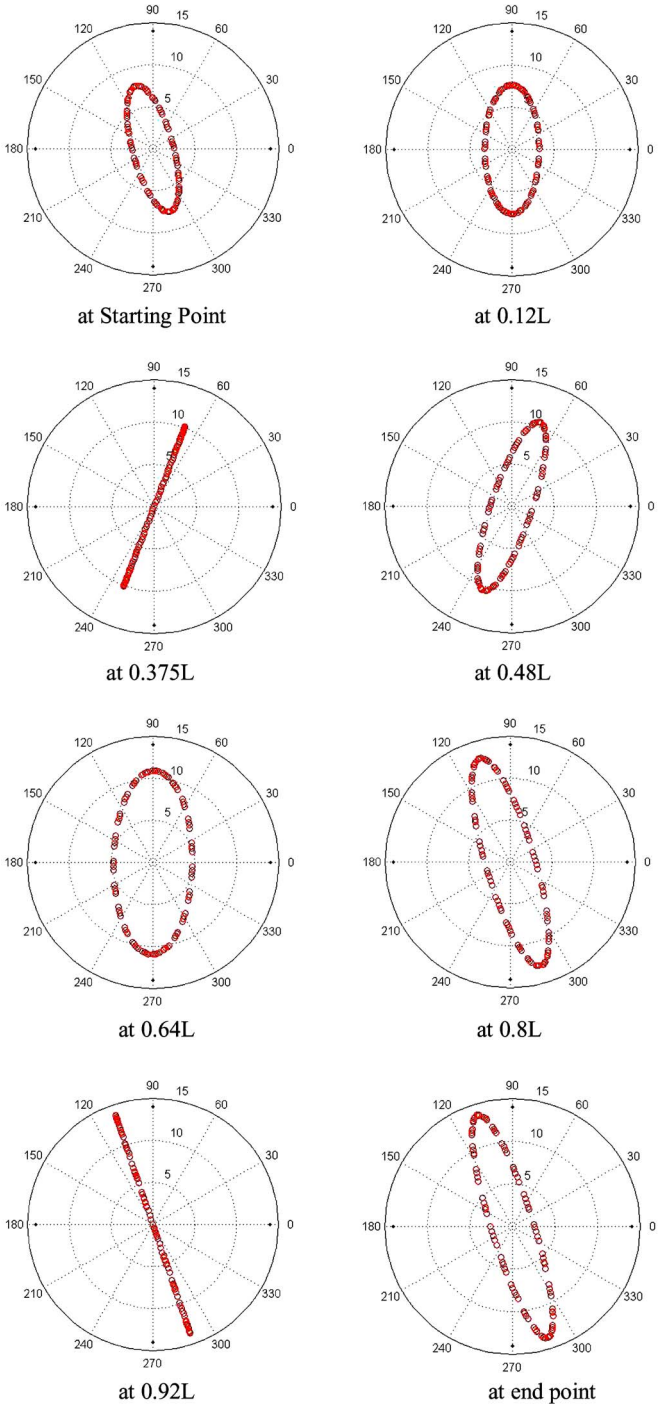

FIG. 2. (Color online) Polarization ellipses of light at various locations inside the ring cavity. L is the cavity length.

stronger or weaker than that along the fast axis. With all the other cavity parameters being fixed and the orientation of the polarizer being so changed that the energy ratio between the two polarization modes was reversed, the phase differences were recalculated and tabulated in Table II. It is evident from the two tables that the strength of cavity linear birefringence has little effect on the accumulated nonlinear phase difference between the two polarization modes, which is mainly determined by the pulse energy ratio along the fast and slow fiber axes.

TABLE I. Phase difference between the two polarization modes accumulated in one cavity round-trip. The pulse energy along the slow axis is roughly 2.5 times that of along the fast axis.

	$L=L_B$	$L=2L_B$	$L=3L_B$	$L=4L_B$
Linear alone	-2π	-4π	-6π	-8π
Actual	−7.000	−13.224	−19.428	−25.665
Discrepancy	+0.717	+0.658	+0.578	+0.532

It is obvious from the results shown above that, to preserve the polarization state of the soliton throughout its propagation in optical fibers, the linear birefringence of the fibers used should be very weak, with the beat length being in the order of ten times that of the length, only in this case, the phase difference between the two polarization components induced by the linear fiber birefringence could be effectively compensated by that caused by the nonlinear birefringence.

V. SOLITON POLARIZATION DYNAMICS

Zhao *et al.* [13,14] showed that, in the fiber soliton lasers if the soliton energy is strong, cavity nonlinear effects will then become prominent, resulting in soliton deterministic dynamics including the soliton period doubling, tripling, and route to chaos. Although the formation mechanism of these phenomena in soliton fiber lasers has been extensively investigated and is relatively clear now, the question of how the polarization states of the solitons evolve in the cavity when they experience period-doubling or tripling bifurcation has not been addressed yet. By applying the same methodology described above, we further investigated the polarization-state evolutions of these solitons.

Figures 3(a) and 4(a) show, for example, the soliton evolution of a fiber laser whose soliton repetition period is doubled and tripled, respectively, compared to the conventional soliton operation described above. Different from the conventional soliton operation, where the soliton returns to its original value after every round of cavity propagation (it can therefore be denoted as a period-1 state), the soliton in the period-doubled or tripled state only returns to its original value after every two or three round-trips of cavity propagation as a result of the laser dynamics. Figures 3(b) and 4(b)

TABLE II. Phase difference between the two polarization modes accumulated in one cavity round-trip. The pulse energy along the fast axis is roughly 2.5 times that of along the slow axis.

	$L=L_B$	$L=2L_B$	$L=3L_B$	$L=4L_B$
Linear alone	-2π	-4π	-6π	-8π
Actual	−5.917	−11.973	−18.260	−24.605
Discrepancy	−0.366	−0.593	−0.590	−0.528

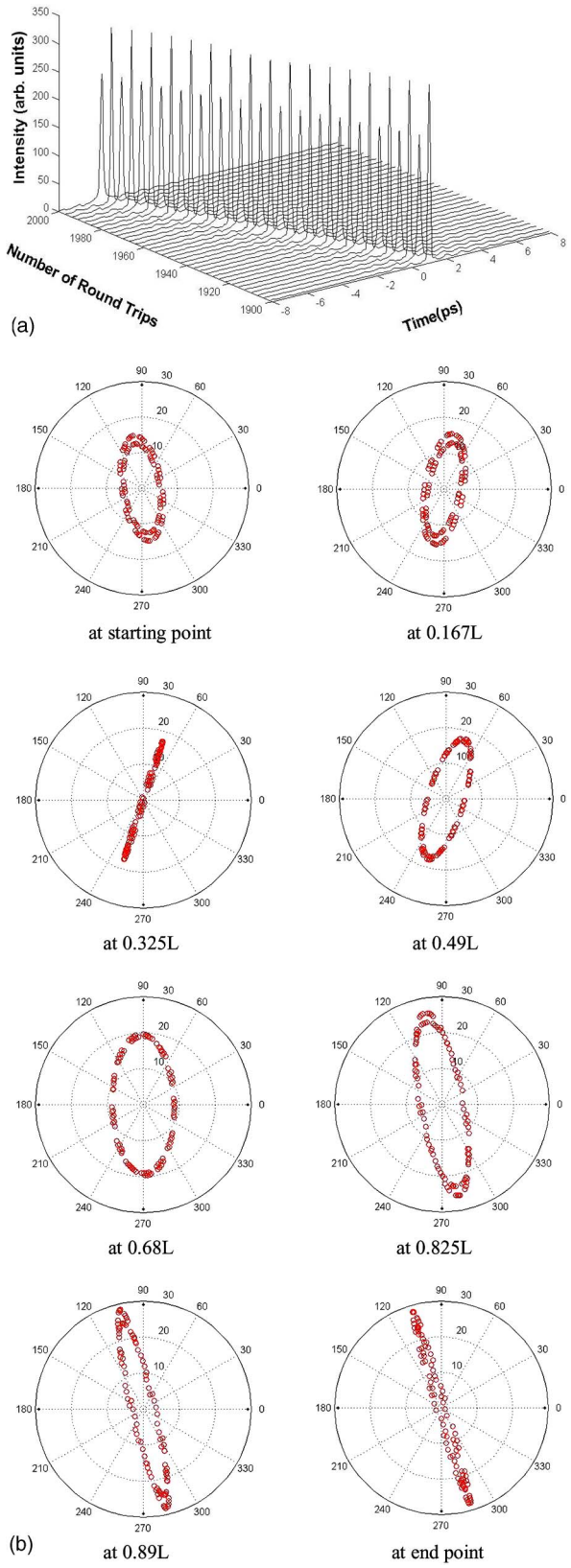

FIG. 3. (Color online) (a) Soliton evolution in a period-doubled state. (b) The corresponding soliton polarization evolution in the cavity. L: cavity length, $L=L_B$.

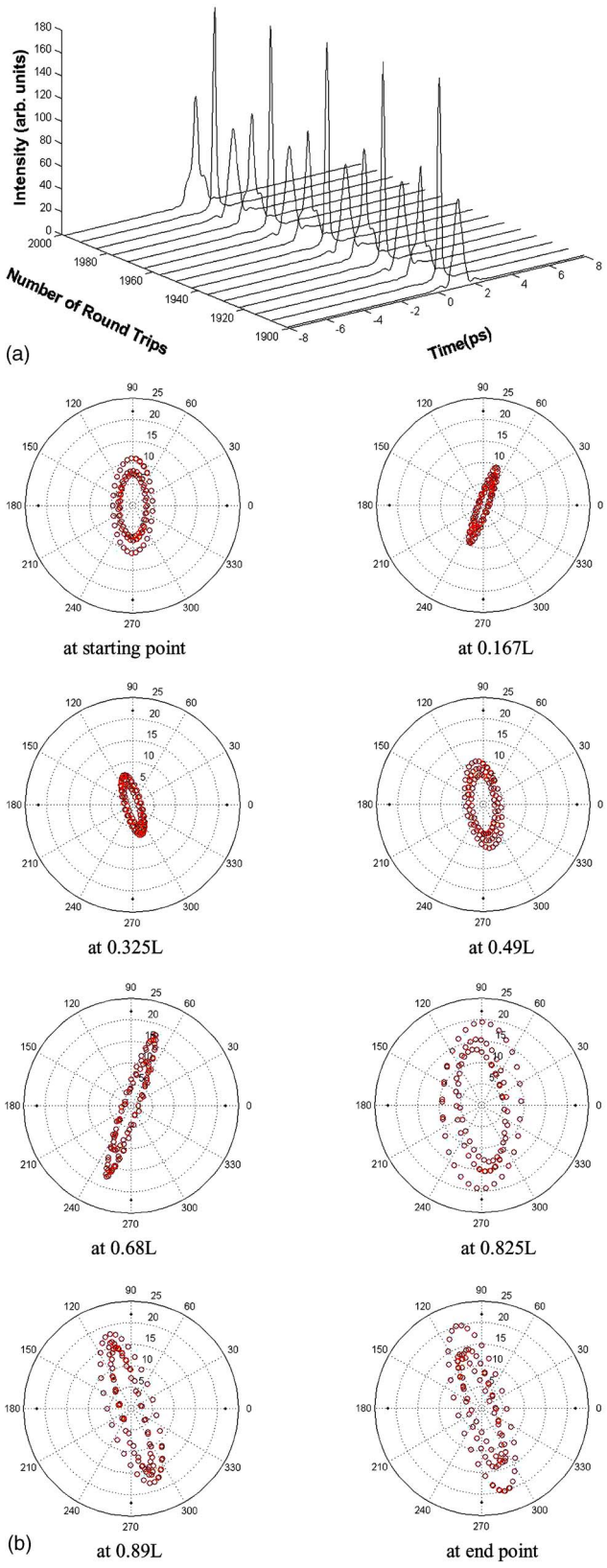

FIG. 4. (Color online) (a) Soliton evolution in a period-tripled state. (b) The corresponding soliton polarization evolution in the cavity. L: cavity length, $L=2L_B$.

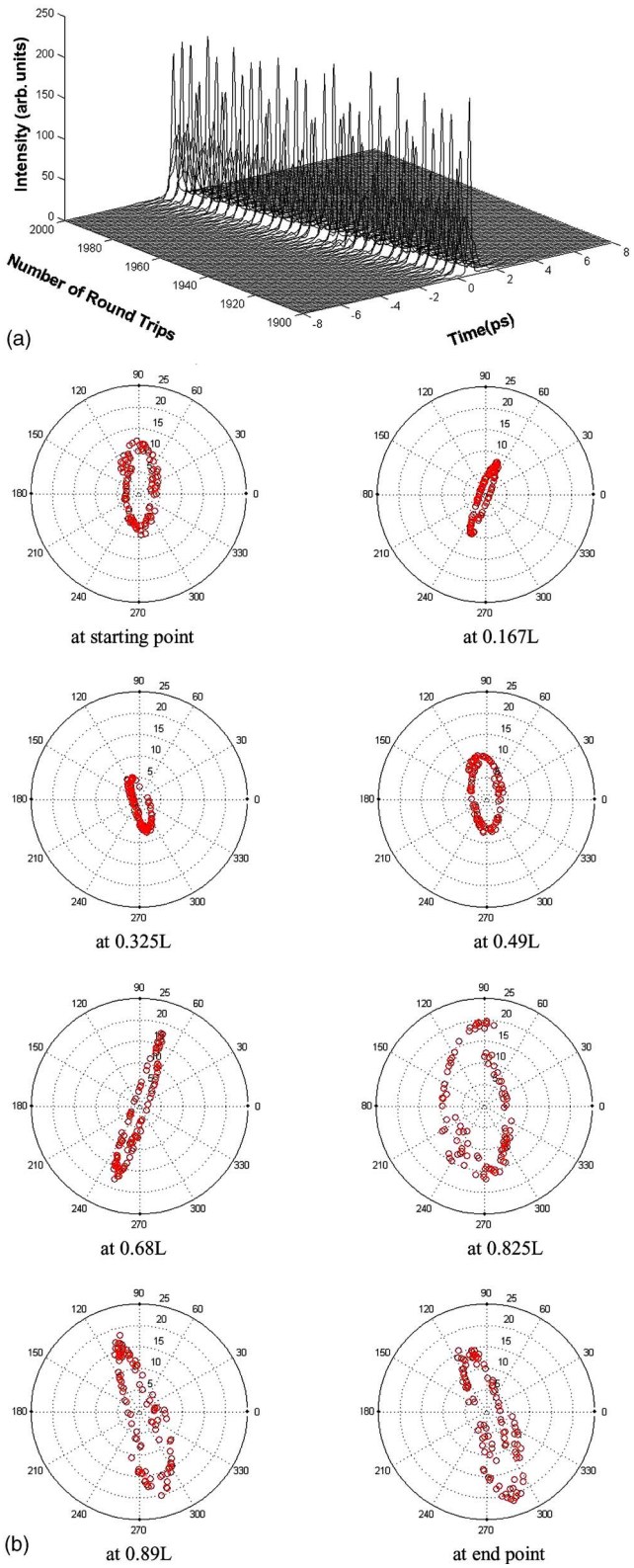

FIG. 5. (Color online) (a) Soliton evolution in a chaotic state. (b) The corresponding soliton polarization evolution in the cavity. L: cavity length, $L=2L_B$.

depict the corresponding soliton polarization-state evolution in the cavity. It was found that in these states the soliton polarization evolution still possesses such general characteristics as those aforementioned for the period-1 state, i.e., the polarization ellipse rotates as the soliton propagates in the cavity, after one period returns to the original one and then repeats, and the number of rounds of the polarization ellipse rotation completed over one cavity length is close to the ratio of the cavity length over the beat length with the discrepancy arisen from the nonlinear birefringence required to achieve and maintain mode-locking. Note that now one period corresponds to two- or three-round-trip time. However, at a fixed position in the cavity the soliton polarization states of the adjacent round-trips are not exactly the same. It can be seen that at a fixed position in the cavity there are two (or three) clear polarization ellipses, and the orientations and ellipticities of them are slightly different. Obviously, the polarization state of the soliton also exhibits the period-doubling (tripling) dynamics despite the fact that there is a polarizer in the cavity, which determines the polarization state of the light immediately after passing through it.

While in the periodic states at a fixed position the tips of the electrical-field vectors can trace out clear polarization ellipses, when chaos was entered [Fig. 5(a)] the profile of the polarization ellipse was no longer well defined as shown in Fig. 5(b). This result suggests that when the soliton emission of a laser becomes chaotic, its polarization at a fixed position in the cavity is no longer fixed, but changes from round-trip to round-trip. This feature of the soliton polarization evolution agrees with the soliton pulse intensity variation in the chaotic state. As shown in Fig. 5(a), at a fixed position in the cavity the soliton intensity varies from round-trip to round-trip. Nonetheless, we note that even in the chaotic state the electrical-field tips still traced out a reasonably elliptical shape, which implies that the round-trip-to-round-trip change of the soliton polarization state was not too large.

VI. CONCLUSION

In this paper, we have explicitly calculated the soliton polarization evolution in a fiber-ring laser passively mode-locked by the NPR technique. By numerically solving the coupled Ginzburg-Landau equations and using the pulse-tracing technique to incorporate the cavity effect in the simulation, we were able to determine and plot the polarization ellipse of the soliton at every position throughout the laser cavity. It was found that in the conventional stable soliton operation, although the soliton polarization varies as it propagates inside the laser cavity, at a fixed position the soliton polarization is fixed, which is invariant with time. This feature can be well understood as it is caused by the intracavity polarizer. The presence of the polarizer in the cavity provides a polarization feedback on the solitons circulating in the cavity. Therefore, the polarization evolution of the soliton is constrained by the laser cavity. It was also shown that when the soliton exhibits deterministic dynamics, its polarization also displays the same dynamics. In this case at a fixed position in the cavity the soliton could have several discrete, fixed polarization states or even no fixed polarization state despite the presence of an intracavity polarizer.

[1] V. J. Matsas, D. J. Richardson, T. P. Newson, and D. N. Payne, Opt. Lett. **18**, 358 (1993).
[2] E. Nelson, D. J. Jones, K. Tamura, H. A. Haus, and E. P. Ippen, Appl. Phys. B **65**, 277 (1997).
[3] N. Duling III, Opt. Lett. **16**, 539 (1991).
[4] A. Gomes, L. Orsila, T. Jouhti, and O. G. Okhotnikov, IEEE J. Sel. Top. Quantum Electron. **10**, 129 (2004).
[5] H. A. Haus, J. G. Fujimoto, and E. P. Ippen, J. Opt. Soc. Am. B **8**, 2068 (1991).
[6] C. J. Chen, P. K. A. Wai, and C. R. Menyuk, Opt. Lett. **17**, 417 (1992).
[7] M. Salhi, H. Leblond, and F. Sanchez, Phys. Rev. A **67**, 013802 (2003).
[8] D. Y. Tang, L. M. Zhao, B. Zhao, and A. Q. Liu, Phys. Rev. A **72**, 043816 (2005).
[9] C. R. Menyuk, IEEE J. Quantum Electron. **23**, 174 (1987).
[10] S. G. Evangelides, L. F. Mollenauer, J. P. Gordon, and N. S. Bergano, J. Lightwave Technol. **10**, 28 (1992).
[11] S. T. Cundiff, B. C. Collings, N. N. Akhmediev, J. M. Soto-Crespo, K. Bergman, and W. H. Knox, Phys. Rev. Lett. **82**, 3988 (1999).
[12] S. T. Cundiff, B. C. Collings, and W. H. Knox, Opt. Express **1**, 12 (1997).
[13] L. M. Zhao, D. Y. Tang, F. Lin, and B. Zhao, Opt. Express **12**, 4573 (2004).
[14] L. M. Zhao, D. Y. Tang, and A. Q. Liu, Chaos **16**, 013128 (2006).
[15] D. C. Hutchings and J. M. Arnold, J. Opt. Soc. Am. B **16**, 513 (1999).
[16] N. N. Akhmediev, A. V. Buryak, J. M. Soto-Crespo, and D. R. Andersen, J. Opt. Soc. Am. B **12**, 434 (1995).
[17] D. N. Christodoulides and R. I. Joseph, Opt. Lett. **13**, 53 (1988).
[18] K. J. Blow, N. J. Doran, and D. Wood, Opt. Lett. **12**, 202 (1987).
[19] B. A. Malomed, Phys. Rev. A **43**, 410 (1991).
[20] M. Salhi, H. Leblond, and F. Sanchez, Phys. Rev. A **68**, 033815 (2003).
[21] G. P. Agrawal, IEEE Photonics Technol. Lett. **2**, 875 (1990).